Published in final edited form as:
Invest Ophthalmol Vis Sci. 2009 November ; 50(11): 5057–5069. doi:10.1167/iovs.08-3232.

Hemi-Retinal Form Deprivation: Evidence for Local Control of Eye Growth and Refractive Development in Infant Monkeys

Earl L. Smith III[1,4], **Juan Huang**[1,4], **Li-Fang Hung**[1,4], **Terry L. Blasdel**[2], **T.L. Humbird**[2], and **K.H. Bockhorst**[3]

[1]College of Optometry, University of Houston, Houston, TX, USA1

[2]Animal Care Operations, University of Houston, TX, USA

[3]University of Texas at Houston Medical School, TX, USA

[4]Vision CRC, Sydney, Australia

Abstract

PURPOSE—To determine whether refractive development in primates is mediated by local retinal mechanisms, we examined the effects of hemi-retinal form deprivation on ocular growth and the pattern of peripheral refractions in rhesus monkeys.

METHODS—Beginning at about 3 weeks of age, 9 infant monkeys were reared wearing monocular diffuser lenses that eliminated form vision in the nasal field (nasal field diffusers, NFD). Control data were obtained from the non-treated fellow eyes, 24 normal monkeys, and 19 monkeys treated with full-field diffusers (FFD). Refractive development was assessed by retinoscopy performed along the pupillary axis and at eccentricities of 15, 30 and 45 deg. Central axial dimensions and eye shape were assessed by A-scan ultrasonography and magnetic resonance imaging (MRI), respectively.

RESULTS—Hemi-retinal form deprivation altered refractive development in a regionally selective manner, typically producing myopia in the treated hemi-fields. In particular, 6 of the NFD monkeys exhibited substantial amounts (−1.81 to −9.00 D) of relative myopia in the nasal field that were most obvious at the 15 and 30 deg nasal field eccentricities. The other 3 NFD monkeys exhibited small amounts of relative hyperopia in the treated field. The alterations in peripheral refraction were associated with local, region-specific alterations in vitreous chamber depth in the treated hemi-retina.

CONCLUSIONS—The effects of form deprivation on refractive development and eye growth in primates are mediated by mechanisms, presumably retinal, that integrate visual signals in a spatially restricted manner and exert their influence locally.

Keywords

myopia; hyperopia; peripheral refraction; refractive error; emmetropization

Many aspects of ocular growth and refractive development are regulated by visual feedback associated with the eye's refractive state (see refs 1 and 2 for reviews). Knowledge of the operational properties of the vision-dependent mechanisms that influence refractive development is critical for understanding the role of vision in the genesis of common refractive errors and for developing the optimal treatment regimens for refractive error.

Corresponding author: Earl L. Smith III, University of Houston, College of Optometry, 505 J Armistead Bldg, Houston, TX 77204-2020, Tel: 713-743-1946; Fax: 713-743-2053; esmith@uh.edu.

In this respect, one of the most important discoveries arising from animal research is that in some species many of the effects of vision on ocular growth and refractive development appear to be mediated by mechanisms that are located entirely within the eye (see refs 2 and 3 for reviews). The primary evidence for these retinal mechanisms has come from reduction-strategy experiments that have examined the effects of a visual stimulus on refractive development when the obvious neural inputs and/or outputs from the eye have been eliminated. For example, in chicks and tree shrews pharmacological blockade and/or surgical section of the optic nerve do not interfere with the phenomenon of form-deprivation myopia (FDM)4–6 or the recovery from FDM7 and although the set point for emmetropization is altered by optic nerve section, compensation for positive and negative lenses still occurs.8,9 Similarly, surgical interruption of the primary parasympathetic inputs to the eye does not prevent FDM or lens induced changes in refractive error in chicks.9 These experiments show that the visual signals that alter eye growth do not have to leave the eye and that the most obvious neural input to the eye is not essential for many aspects of vision-dependent ocular growth.

In addition, it has been shown that these retinal mechanisms exert their influence in a spatially restricted, local manner. The most direct evidence for the local nature of these retinal mechanisms come from experiments in which the nature of visual experience has been varied across the visual field. For example, in chicks, tree shrews and guinea pigs that are reared with diffusers or negative lenses that only cover part of the visual field, the axial elongation and myopia are restricted to the affected part of the retina (McFadden, IOVS, 2002, 43, E-Abstract 189).10–14 Similarly, in chicks positive lenses that only affect the image over half the retina slow vitreous chamber elongation and produce hyperopia only in the treated portion of the retina.10 These results demonstrate that the ocular mechanisms that regulate eye growth pool visual signals from restricted spatial regions and exert their influence locally. It is thought that the actions of these local retinal mechanisms alter the shape of the eye in response to variations in the environment in order to enhance the optimum focus across the retina.1,13,15,16

It is not known if local retinal mechanisms are involved in emmetropizing responses in primates. In a study involving a small number of monkeys, Raviola and Wiesel17 found that optic nerve section prevented FDM in stumptail macaques, but not in rhesus monkeys. In addition, surgically eliminating the parasympathetic and sympathetic inputs to the eye did not prevent FDM in rhesus monkeys.17 These results suggest that there are vision-dependent retinal mechanisms in rhesus monkeys that influence eye growth, but not in stumptail monkeys. This discrepancy between two closely related species is puzzling and may have come about as a result of the variability associated with the phenomenon of form-deprivation myopia in monkeys,18–21 possible hyperopic shifts produced by optic nerve section,9 and/or the small number of animals studied. Regardless, it has not been clearly established that refractive development is mediated by retinal mechanisms in primates and there have not been any previous attempts to characterize the spatial summation properties of any potential retinal mechanisms in primates. Because of the significance of local retinal mechanisms to our understanding of the effects of vision on refractive development, it is critical to determine if they exist in primates and if they can produce predictable changes in eye shape. The great majority of what we know about local retinal mechanisms comes from studies in chicks. However, because of differences in the structure of the sclera in chicks and primates,3 it is not reasonable to expect that similar visual manipulations will produce comparable shape changes in chicks and primates. For example, the cartilaginous portion of the chick sclera is comparatively rigid and depriving half of the retina of a chick produces a prominent bulge on the deprived side of the eye.5,13 Because primates have a less rigid fibrous sclera, it is possible that providing half of the retina with a stimulus for growth would produce a more symmetrical, prolate axial elongation in primates.

In this study, we employed a rearing strategy that has provided strong evidence for the existence of local retinal mechanisms in chicks, guinea pigs, and tree shrews. Specifically, we examined the effects of hemi-retinal form deprivation on ocular growth and the pattern of peripheral refraction in infant monkeys. Some of these results have been presented in abstract form.22

MATERIALS AND METHODS

Subjects

Data are presented for 56 infant rhesus monkeys (*Macaca mulatta*) that were obtained at 1 to 3 weeks of age and housed in our primate nursery that was maintained on a 12-hour light - 12-hour dark lighting cycle. All of the rearing and experimental procedures were reviewed and approved by the University of Houston's Institutional Animal Care and Use Committee and were in compliance with the ARVO Statement for the Use of Animals in Ophthalmic and Vision Research.

The primary subjects were 9 infant monkeys that were reared wearing goggle-mounted, nasal visual field diffusers (NFDs) over one eye and clear, zero-powered lenses in front of the fellow eye (see ref 23 for details of our goggle rearing method). The NFDs consisted of a zero-powered carrier lens that was partially covered with a commercially available occlusion foil (Bangerter Occlusion Foils, Fresnel Prism and Lens Co.). The occlusion foils (the manufacturer's designation "LP" for "light perception") were the strongest diffusers that we employed in our previous studies of form deprivation myopia in monkeys.19 These diffusers, which act as high spatial frequency filters, reduced the contrast sensitivity of normal adult humans by over 1 log unit for grating spatial frequencies of 0.125 cycles/degree with a resulting cut-off spatial frequency near 1 cycle/degree. The vertical border of the occlusion foil was positioned approximately 1 mm to the temporal side of the center of the treated eye's entrance pupil while the eye was in primary gaze and, thus, degraded form vision throughout the nasal visual hemi field while allowing good central vision and unrestricted vision in the temporal visual hemi field. Without the occlusion foils, the carrier lenses provided monocular and binocular fields of view in the horizontal plane of 80 and 62 degrees, respectively, and an 87 degree vertical field. The NFDs typically occluded slightly more than half of the treated eye's monocular field. The lens-rearing period, which extended from about 3 weeks of age (22 ± 3 days) until 5–6 months of age (172 ± 15 days), encompassed the bulk of the rapid phase of emmetropization in rhesus monkeys.24

For comparative purposes, data are also presented for 19 monkeys that were subjected to full-field monocular form deprivation (FFD) using the same "LP" diffusers that were used to construct the NFDs. The FFD monkeys wore the diffuser lenses continuously from 23 ± 3 to 150 ± 20 days of age. The data for all of the FFD monkeys have been presented in previous publications.19,20,25

Control data for central refractive errors and axial dimensions were obtained from 24 normal animals reared with unrestricted vision and 4 animals that were reared with clear, zero-powered lenses over both eyes (age = 145 ± 9 days of age).5,13,19,23,24,26–28 Control data for peripheral refractions were obtained from 7 of the normal animals (age = 162 ± 11 days of age); the data for 6 of these normal monkeys have been previously reported).25,29

Ocular Biometry

The basic details of our biometric measurements have been described elsewhere.23,29 Briefly, to obtain the ocular measurements, each animal was anesthetized (ketamine hydrochloride, 15–20 mg/kg: acepromazine maleate, 0.15–0.2 mg/kg) and cycloplegia was induced using 1% tropicamide.

Central and peripheral, spherical-equivalent refractive errors were measured by streak retinoscopy by two well-practiced investigators and averaged30 (details of our methods are described in references 25 and 29) Central refraction was determined along the pupillary axis (i.e., the first Pukinje image produced by the retinoscope beam was observed in the center of the subject's entrance pupil). Following measurements of the central refraction, retinoscopy was performed at 15° intervals along either the vertical or horizontal meridians out to a maximum eccentricity of 45°. Throughout the paper, the eccentricities for refractive errors are specified with respect to the visual field (e.g., temporal field measurements correspond to refractive errors for the nasal retina).

Although peripheral retinoscopy is often complicated by the phenomenon of "scissoring" or the so called "double sliding-door effect", using the criteria proposed by Rempt et al.,31 the measures were reasonably repeatable. For example, the average limits of agreement obtained for repeated retinoscopic measures in young monkeys were 1.06, 1.03, and 1.21 D for the 15°, 30°, and 45° eccentricities, respectively.29

Ocular axial dimensions were measured by A-scan ultrasonography implemented with either a 7- (Image 2000; Mentor, Norwell, MA) or 12-MHz transducer (OTI Scan 1000; OTI Ophthalmic Technologies, Inc, Ontario, Canada). Intraocular distances were calculated from the average of 10 separate measurements using velocities of 1532, 1641, and 1532 m/sec for the aqueous, lens, and vitreous, respectively. Corneal curvature was measured with a hand-held keratometer (Alcon Auto-keratometer; Alcon Systems Inc, St Louis, MO) and/or a videotopographer (EyeSys 2000; EyeSys technologies Inc, Houston, TX). Both instruments provided repeatable and comparable measures of central corneal curvature in infant monkeys.32

The biometric measurements were initially obtained at ages corresponding to the onset of lens wear and then at approximately two week intervals thereafter. Due to time constraints, peripheral refractions were obtained on either the horizontal or vertical meridians during a given session.

Magnetic Resonance Image Acquisition

Near the end of the diffuser-rearing period (about 160 days of age), magnetic resonance imaging (MRI) was performed on the NFD-reared animals using a 7T Bruker Biospec horizontal bore scanner (USR70/30; Bruker, Karlsruhe, Germany). The details of our MRI procedures have been described previously.25 Comparison data were obtained from 2 age-matched normal monkeys and 6 animals that were treated with full-field "LP" diffusers. The comparison data have been previously reported.25

The MRI scans were performed while the animals were anesthetized with 2% isoflurane gas anesthesia, which greatly reduced residual eye movements in our infant monkeys.25 During the MRI scans the monkeys were held in a supine position. The animal's head was fixed on a custom-designed head holder so that their face was parallel to the floor with their eyes looking in the upward direction so that the eyes' optical axes were approximately perpendicular to the bore of the magnet. The initial tripilot scan was used to localize the position of the monkey's eyes. The magnetic field homogeneity was then optimized using localized shimming with a point-resolved spectroscopy (PRESS) procedure. The anatomical images were acquired using a 3D-rapid acquisition paradigm with a relaxation enhancement (RARE) sequence. T2-weighted images were obtained with long repetition (TR, 1500 ms) and effective echo times (TE, 96 ms) in order to enhance the contrast between the fluids and tissues of the eye. The spatial resolution of the images was 0.195 × 0.195 × 0.5 mm in the horizontal plane.

The acquired axial MR images were reconstructed via in-house software developed using Matlab, which allowed the MR images to be viewed from axial, sagittal and coronal directions. The software interpolated between the axial image slices to produce a uniform resolution of 0.195 mm in the three dimensional matrix, which, in terms of vitreous chamber depth, corresponds to a dioptric interval of about 1 D. To ensure that measurements were obtained from the appropriate image plane, the three dimensional volumes were rotated so that when viewed from the sagittal direction, the line connecting the equatorial poles of the lens was vertical in the superior-inferior direction. This was done to ensure that the approximate optical axis was within the axial or horizontal plane. A Canny edge detection algorithm was applied to the horizontal plane of the rotated images to determine the boundaries between ocular structures. The approximate optical axis was defined as the perpendicular in the horizontal plane through the midpoint of the line connecting the equatorial poles of the lens. The horizontal slices that contained the greatest lens thicknesses were used for all further measurements. The intersection of the presumed optical axis and the posterior lens surface was considered as the approximate position of the second nodal point and was used as the reference for specifying retinal eccentricities. The primary measure of interest was the vitreous chamber depth, which was defined as the distance between the approximate position of the second nodal point and the retina. Vitreous chamber depth was determined as a function of eccentricity in 15° intervals out to eccentricities of 45° using the approximate position of the posterior nodal point as a reference.

Statistical Analysis

Repeated-measures ANOVAs (SuperANOVA; Abacus Concepts, Inc, Berkeley, CA) and multiple comparisons were used to compare the symmetry of refractive errors along the horizontal and vertical meridians in a given eye and to determine if there were differences in refractive error as a function of eccentricity or differences in the patterns of peripheral refraction between eyes. Mixed-design, repeated-measures ANOVAs were used to determine if there were differences between subject groups in refractive error or relative vitreous chamber depth. Probability values were adjusted using Geisser-Greenhouse corrections. Linear regression analyses of the relationship between vitreous chamber depth and refractive error were performed using Minitab software.

RESULTS

Early onset, full-field form deprivation typically produces central axial myopia in young monkeys. However, as illustrated in Figure 1A, even with consistent, severe form deprivation, the degree of myopia varies substantially between animals, with some animals developing relative hyperopia in their treated eyes.

The NFDs also interfered with central refractive development. Like full-field form deprivation, the NFDs produced a large range of central refractive errors. At the end of the treatment period, the anisometropias in the NFD-reared animals ranged from +1.81 to −9.94 D. Although 5 of the NFD monkeys exhibited small amounts of relative central hyperopia in their treated eyes, 4 of the 9 treated monkeys showed substantial amounts of myopia along the pupillary axes of their treated eyes. The central myopia found in these NFD monkeys was due to increases in the vitreous chamber depth of the treated eyes and the relationship between the degree of anisometropia and the interocular differences in vitreous chamber depth in NFD-reared monkeys was similar to that found in animals reared with full-field form deprivation (Figure 1B). As a group, there were no interocular differences in corneal power ($T = 0.55$; $P = 0.60$) or corneal asphericity between the treated and fellow eyes of the NFD monkeys ($T = 0.66$; $P = 0.53$). However, the corneas in the treated eyes of the 4 NFD monkeys that exhibited central myopia were on average 0.56 D steeper than the corneas of their fellow eyes ($T = 3.64$; $P =$

0.04), but there was no systematic interocular differences in asphericity Q values ($T = -0.88$; $P = 0.44$)

More importantly, several observations indicated that the NFDs produced localized, regionally selective changes in refractive error. First, the NFDs consistently produced asymmetries in the pattern of peripheral refractions in the horizontal meridian. Figure 2 shows longitudinal data, specifically spherical-equivalent refractive corrections plotted as a function of horizontal eccentricity, for the treated (filled circles) and fellow eyes (open circles) of 5 representative monkeys reared with the NFDs. At the onset of the treatment period, the absolute central refractive errors and the patterns of peripheral refraction were very well matched in the two eyes of the NFD monkeys ($F = 0.01$, $P = 0.91$). Specifically, all of the experimental animals exhibited moderately hyperopic central refractive errors and there was a tendency for the eyes to be less hyperopic in the periphery, particularly in the nasal field. Moreover, there were no differences in the absolute central and peripheral refractive errors between the treated eyes of the NFD monkeys and the right eyes of the normal animals ($F = 1.54$, $P = 0.24$).

With time, the non-treated, fellow eyes of most of the NFD monkeys exhibited changes in refractive error that were indicative of emmetropization, however, the treated eyes demonstrated clear departures from the normal emmetropization process that were most obvious in the nasal field. As illustrated by the plots in the top two rows of Figure 2, the treated eyes of 3 of the NFD monkeys developed relative hyperopic refractive errors in their nasal visual fields. These changes, which were first manifest as a relative hyperopia in the treated eye's nasal field and as interocular refractive-error differences in the nasal field, were apparent at the first measurement session after the onset of lens wear (typically 14 days). Although the relative nasal-field hyperopic refractions were small in these monkeys, the interocular differences in the nasal field were consistent throughout the treatment period and the degree of relative hyperopia in the treated eyes generally increased in magnitude with time.

Six of the 9 NFD-reared monkeys developed relative myopic errors in the nasal field. As illustrated by the representative data in the lower 3 rows of Figure 2, refractive development in the temporal fields of the treated eyes was largely unaffected throughout the treatment period. However, the NFDs produced obvious myopic errors in the nasal fields of most treated eyes. The resulting nasal-temporal asymmetries in refractive error in the treated eyes were noted within 30 days of the onset of lens wear and the degree of myopia in the nasal field, and consequently the nasal-temporal asymmetries, increased during the treatment period. Although the refractive errors along the pupillary axis were affected in most of these monkeys, the observed myopic refractive errors were typically larger at either the 15° or 30° nasal field eccentricities.

The relative peripheral refractive errors measured along the horizontal meridian at the end of the treatment period for all of the NFD monkeys are illustrated in Figure 3. The data for the treated (filled symbols) and fellow eyes (open symbols) have been normalized to the refractive error measured at 45° in the temporal field. The shaded region represents ±1 SD from the means for the right eyes of the 7 normal monkeys. Typically peripheral refractions are plotted relative to the central refraction, however, we chose to use the 45° temporal eccentricity as a reference because the central refractions were altered in many NFD animals and the absolute differences between the fellow and treated eyes and between treated and normal monkeys were smallest at the temporal 45° eccentricity.

The results in Figure 3 emphasize that the NFDs selectively produced relative myopia in the nasal fields of the majority of the treated eyes. For the animals represented in Figures 3 D–I (the lower row and in the last 2 plots on the right of the upper row), the treated-eye data were in or near the ±1 SD normal zone in the temporal field, but were consistently well below the

normal zone (i.e., more myopic) in the nasal field with the greatest departures from normal occurring at the 15° and 30° nasal field eccentricities. For the other 3 NFD monkeys (Figure 3A–C) the treated-eye data were, with a few exceptions, within the ±1 SD boundaries for the normal animals. However, it is interesting that for two of these animals (Fig 3A, MKY GEN 359; Fig 3B. MKY MIT 367), the pattern of peripheral refractions in the fellow eyes deviated more from the normal monkey data than the data for their treated eyes. Specifically, the fellow eyes were more myopic than normal at the 15° and 30° nasal eccentricities for both of these animals and at the nasal 45° eccentricity for MKY MIT 367.

A repeated-measures ANOVA confirmed that at the end of the treatment period there were significant nasal-temporal asymmetries in the peripheral refractions in the treated eyes of the NFD monkeys ($F = 34.43$, $P = 0.003$), but not in the fellow eyes ($F = 0.07$, $P = 0.42$). In addition, there were significant eccentricity dependent differences in the absolute peripheral refractions between the treated eyes of the NFD monkeys and the right eyes of the normal monkeys ($F = 4.85$, $P = 0.0003$).

The interocular differences in peripheral refractions for individual animals also emphasized the selective effects of the NFDs. In Figure 4, the interocular differences in refractive error obtained at the end of the treatment period are plotted as a function of eccentricity for individual treated monkeys (open symbols). The filled symbols represent the mean interocular differences for 7 normal age-matched monkeys; the shaded area demarcates ±2 SDs from the means. The left and right eyes of the normal monkeys were well matched at all eccentricities. However, the interocular difference plots for the treated monkeys showed obvious nasal-temporal asymmetries ($F = 23.09$; $P = 0.0001$). At the 45° temporal field eccentricity, the data for all of the treated animals fell within the ±2 SD region for the normal monkeys. However, as one moves from the temporal to the nasal field, the interocular differences in refractive error generally increased with the greatest differences being found at or near the 15° nasal field eccentricity. For 5 of the NFD monkeys, the nasal field data for the treated eyes were more myopic than that for their fellow eyes and the interocular differences fell outside the ±2 SD region for the normal monkeys at the nasal 15° and 30° eccentricities. For 2 other NFD animals, the treated eyes were more hyperopic than their fellow eyes at the 15° and 30° nasal field eccentricities and these differences were also more that 2 SDs away from the mean differences for normal monkeys. As noted above, the relative interocular hyperopic anisometropia observed in the nasal fields for these monkeys reflects the fact that their fellow non-treated eyes were more myopic than the eyes of the control monkeys in the nasal visual field.

A comparison of the pattern of peripheral refractions in the vertical and horizontal meridians of the treated eyes also showed that the NFDs produced regionally selective alterations in peripheral refractions. Figure 5 shows refractive error plotted as a function of eccentricity for the horizontal (left) and vertical meridians (middle) of the treated (filled symbols) and fellow eyes (open symbols) for the 4 NFD monkeys that developed relatively large amounts of nasal field myopia (Note that the horizontal- and vertical-meridian data were obtained at similar, but not identical, ages.). In each monkey, the treated eyes were more myopic than their fellow eyes along both their vertical and horizontal meridians. However, in every case the largest amounts of myopia in the vertical meridian were found along the pupillary axis and the degree of myopia decreased in a systematic and relatively symmetric manner in both the superior and inferior fields. As shown in the right column, the interocular differences in refractive error were more symmetrical about the central refraction in the vertical meridian than in the horizontal meridian. Moreover, in every case, the nasal field was more myopic than either the superior or inferior fields. On the other hand, the temporal field tended to be more hyperopic than either the superior or inferior fields, particularly at the 15° and 30° eccentricities. Repeated measures ANOVAs showed that the interocular difference in peripheral refraction in these four monkeys varied with eccentricity in both the horizontal and vertical meridians (horizontal, $F = 14.80$, $P = 0.004$;

vertical, $F = 8.74$, $P = 0.02$). However, multiple comparisons showed that there were significant asymmetries between the nasal and temporal fields ($F = 49.78$, $P = 0.001$), but not between the superior and inferior fields ($F = 2.18$, $P = 0.15$).

The MRI scans showed that the NFDs altered the shape of the treated eye's posterior globe. Figure 6 shows the horizontal MR images obtained at ages corresponding to the end of the treatment period for both eyes of a monkey reared with unrestricted vision (top), a monkey with form-deprivation myopia produced by full-field diffusers (FFDs) (middle), and a NFD monkey that exhibited a large amount of nasal field myopia (bottom). The white lines in each image represent the presumed optical axes and the projections employed to determine vitreous chamber depth at the 15°, 30° and 45° eccentricities. The graphs in the right column show vitreous chamber depth plotted as a function of retinal eccentricity; the treated (or right) and fellow (or left) eyes are represented by the filled and open circles, respectively. For the control animal, inspection of the MRIs reveals that the two eyes had similar shapes and, as illustrated in the figure on the right, the vitreous chamber depths in the left and right eyes were very similar with both eyes showing small systematic increases in vitreous chamber depth from the nasal to temporal hemi retinas. Full-field form deprivation produced an obvious increase in the size of the treated eye; the relative increases in vitreous chamber depth were largest in the treated eye's central retina, but were observed at all eccentricities and were relatively symmetrical in the nasal and temporal hemi retinas. On the other hand, the MRIs from the NFD animal show differences in the shapes of the posterior globe between the treated and fellow eyes. Whereas the contour of the vitreo-retinal interface in the fellow eye was regular and the variations in vitreous chamber depth with eccentricity were similar to those found in the control animal, the treated eye exhibited obvious departures from this normal contour that started just nasal to the central retina and that were associated with an obvious outward bulging of the temporal vitreous chamber.

Figure 7 shows the horizontal MR images obtained near the end of the treatment period for 5 representative NFD monkeys (left column). The treated eyes are shown on the left. The graphs in the right column show the interocular differences in refractive error (open symbols, left ordinate) and vitreous chamber depth (filled symbols, right ordinate) plotted as a function of horizontal eccentricity. Negative numbers on the y-axis indicate that the treated eye was more myopic and had a deeper/longer vitreous chamber than its fellow eye.

For each of the NFD animals there was a close correspondence between the interocular differences in vitreous chamber depth and refractive error, particularly with respect to the pattern of the nasal-temporal asymmetries. For example, the data in the top row of Figure 7 are from a NFD monkey that exhibited small amounts of relative hyperopia in the nasal field of its treated eye. Although on inspection, the MR images revealed that the treated and fellow eyes were similar in shape, quantitative measurements showed that the nasal vitreous chamber (temporal field) in the treated eye was slightly longer than that in the fellow eye and that the interocular differences in vitreous chamber depth decreased systematically in the direction of the temporal retina (nasal field), paralleling the refractive-error data. As illustrated in the lower 4 panels of Figure 7, there were visible interocular differences in the shapes of the posterior globe in the animals with large amounts of nasal visual field myopia and the similarities in the shapes of the interocular difference functions were particularly impressive. In each of these animals, there were little or no interocular differences in refractive error or vitreous chamber depth in the nasal retina / temporal field. There was a steep transition between the nasal and temporal portions of the functions that included the data along the pupillary axis. The interocular differences in vitreous chamber depth and refractive error were greatest in the near temporal retina / nasal visual field and decreased thereafter with increasing eccentricities. The similarities in the shapes of these functions indicate that the nasal-temporal asymmetries in refractive error were due to changes in the shape of the posterior globe. However, differences

in corneal and, possibly, lens power did contribute to the relative vertical positions of the interocular differences functions. For example, the treated-eye cornea of MKY FIN 356 (top row) was 0.59 D flatter than that of the fellow eye, whereas the treated-eye cornea of MKY KIM 364 (fourth row) was 0.88 D steeper than that of its fellow eye. In both cases, compensating for these interocular differences in corneal power would shift the interocular difference curves closer together along the vertical axis. Although the degree of astigmatism increased systematically with eccentricity in both the treated and fellow eyes, we did not observe any nasal-temporal asymmetries in astigmatism that could have contributed to the nasal-temporal asymmetries in spherical-equivalent refractive.

Regression analysis confirmed that the interocular differences in refractive error were due primarily to interocular differences in vitreous chamber depth. Figure 8 shows the interocular differences in refractive error plotted against the interocular differences in vitreous chamber depth for all of the peripheral measurements obtained along the horizontal meridian for all of the NFD-reared monkeys. The local interocular differences in refractive error were significantly correlated with local interocular differences in vitreous chamber depth with an r^2 value of 0.74 ($F = 175.9$, $P < 0.0001$). Although the relationship between refractive error and axial length is not linear, the slope of the best fitting function (5.03 D per mm change in vitreous chamber) agrees well with predictions based on schematic eyes. For example, the average axial length of the fellow eyes at the end of the treatment period was 16.99 mm. Assuming that the distance between the retina and the second principal plane was 91% of the eye's axial length,24 the predicted change in refractive error produced by a 1 mm change in vitreous chamber depth would be 5.6 D.

Although there were some similarities in the alterations in the pattern of peripheral refractions and the shape of the posterior globe produced by FFDs and NFDs, there were also significant differences. Figure 9 compares the effects of FFDs and NFDs. The left column shows average (±SE) data for 6 monkeys that developed at least 1 D of central myopic anisometropia in response full-field form deprivation. The data for the 4 NFD monkeys that showed the largest amounts of induced myopia are shown in the middle column. These NFD animals were selected because the degree of central myopic anisometropia was very similar to that in the FFD monkeys (−6.26 D *vs*. −6.63 D). The fellow eyes of the FFD and NFD monkeys tended to be slightly more hyperopic than the average normal monkey (cross-hatched area in the top row). However, there were no systematic differences between the fellow eyes of the FFD and NFD monkeys in absolute refractive error ($F = 0.29$; $P = 0.60$) or the pattern of relative peripheral refractive errors ($F = 0.51$; $P = 0.62$). On the other hand, there were clear and substantial differences between the treated and fellow eyes of the FFD and NFD monkeys and, regardless of which measure is considered (i.e., refractive errors, top and middle; or interocular differences in vitreous chamber depth, bottom), these interocular differences varied with eccentricity, with both the FFD ($F = 4.40$ to 54.22; $P = 0.006$ to 0.08) and NFD monkeys ($F = 89.18$ to 339.74; $P < 0.0009$) showing larger myopic changes in the nasal field. However, there were significant eccentricity dependent differences in the results for the NFD and FFD monkeys (ametropia, $F = 6.57$; $P = 0.005$; anisometropia, $F = 6.34$; $P = 0.007$; IOD vitreous chamber depth, $F = 3.30$; $P = 0.05$). For example, whereas the absolute refractive errors and the interocular differences in refractive error and vitreous chamber depth at the 15°, 30° and 45° nasal field eccentricities were similar in the FFD and NFD monkeys, these measures at the 15°, 30° and 45° temporal field eccentricities were consistently smaller in the NFD monkeys. As a consequence, as illustrated in the right column of Figure 9, the nasal-temporal asymmetries in absolute refractive error ($F = 13.81$; $P = 0.006$), anisometropia ($F = 12.30$; $P = 0.008$), and interocular differences in vitreous chamber depth ($F = 5.81$, $P = 0.04$) were significantly larger in the NFD monkeys at all the eccentricities that we investigated. The between group differences in temporal field refractive errors can be attributed primarily to differences in the depths of the nasal vitreous chamber. For example, at the 15°, 30° and 45° temporal field

eccentricities, the differences in anisometropia between the FFD and NFD monkeys were 2.92, 2.71, and 1.59 D, respectively. The corresponding differences in the relative vitreous chamber depths were 0.54, 0.42, and 0.27 mm, respectively, which based on model eye calculations (5.6 D / mm), would account for 3.04, 2.36, and 1.51 D of the differences in anisometropia between the NFD and FFD monkeys.

DISCUSSION

The main findings of our study were that 1) hemi-retinal form deprivation altered refractive development in a regionally selective manner, typically producing myopia in the treated hemi-fields of infant monkeys and 2) that these treatment-induced changes in refractive error were associated with local, region-specific alterations in vitreous chamber depth in the treated hemi-retina. In many respects the effects of NFDs were similar to those produced by full-field form deprivation. With both manipulations there is substantial variability in the degree of myopia between animals and the refractive-error changes are axial in nature. The primary difference between the effects of NFDs and FFDs was that the alterations produced by the NFDs were restricted primarily to the treated hemi-retina.

This pattern of results has important implications for the nature of the vision-dependent mechanisms that influence ocular growth and refractive development in primates. As discussed in previous studies involving chickens,5,10,13 many of the global mechanisms that have been frequently hypothesized to mediate the effects of vision on refractive development can not easily explain these selective, local alterations in refractive development. For example, it is difficult to imagine how accommodative mechanisms or overall alterations in intraocular pressure could produce the observed nasal-field myopia. Instead, in conjunction with Raviola and Wiesel's observation that optic nerve section does not prevent form deprivation myopia in rhesus monkeys,17 our results provide strong support for the idea that the effects of vision in primates are dominated by mechanisms that are located entirely within the eye, that integrate information in a spatially restricted manner, and that exert their influence selectively on the subjacent sclera. As hypothesized by previous investigators, the presence of these local retinal mechanisms could regulate the shape of the globe during early development to optimize refractive error across the retina.13,15,16 We have recently provided evidence that indicates that emmetropization occurs in the peripheral as well as the central retina in infant primates. 29 It is reasonable to suppose that the local retinal mechanisms revealed in this study mediate this overall emmetropization process in young monkeys. However, it is important to keep in mind that our results are limited to form deprivation. Because the mechanisms that mediate the effects of form deprivation and optical defocus may not be identical,33 it will be important to determine whether hemi-retinal changes in refractive development can also be produced by optically imposed defocus.

Little is known about the spatial integration properties of local retinal mechanisms. In particular, it would be valuable to know the effective summation areas of these mechanisms and if they change with eccentricity. In many respects, the NFDs employed in this study can be considered an edge stimulus and the changes in vitreous chamber depth and refractive error between the nasal and temporal hemi-retinas of our NFD-reared monkeys represent functional edge spread functions for local retinal mechanisms in the central retina. In this respect, the interocular difference plots for refractive error and vitreous chamber depth in Figure 7 and the peripheral refraction plots in Figure 2 provide a rough estimate of the upper limits of the lateral spread of the activity associated with local retinal mechanisms, at least those located near the fovea. For example, for the NFD-reared monkeys that developed relatively large amounts of nasal field myopia, the transition between affected and apparently normal retina occurs over about 30 degrees of the retina and the width of the normalized edge functions at half height is approximately 20 degrees. In other words, the influence of these mechanisms falls by 50%

over about 3–4 mm along the horizontal meridian of the retina (depending on age and eye size). Of course, these estimates do not take into account the potential "blurring" effects produced by the optics of the eye and, particularly, by eye movements. Consequently, it is likely that the effective zones of influence of these local retinal mechanisms are smaller than these estimates.

In both hemi-fields of the FFD monkeys and in the nasal hemi-field of the NFD monkeys the degree of induced myopia declined at the larger eccentricities. The resulting relative peripheral hyperopia reflects changes in the shape of the posterior globe. Specifically, in both FFD and NFD monkeys, the treated hemi-retina became less oblate / more prolate in shape. It is possible that these shape changes reflect a decrease in the ability of local mechanisms in the periphery to influence ocular shape. Regardless, the results indicate that relative peripheral hyperopia may be a consequence or side effect of central axial elongation.

The observed hemi-field changes in the refractive errors of our infant monkeys are qualitative similar to those produced by hemi-retinal form deprivation in chicks,5,11,13 tree shrews,14 and guinea pigs (McFadden, IOVS, 2002, 43, E-Abstract 189), and, thus, provide another example of how the fundamental operational properties of the vision-dependent mechanisms that regulate refractive development have been conserved across species. Given the dominance of the fovea in primate vision, one might have expected that in comparison to species with more homogenous retinas, local retinal mechanisms would be less conspicuous in primates and that refractive development would be dominated by central vision. However, as we have previously demonstrated central vision is not essential for many aspects of vision-dependent ocular growth and peripheral vision can dominate central refractive-error development in primates.28,34 The presence of local retinal mechanisms in monkeys provides a mechanistic explanation for the impact of peripheral vision on primate refractive development. Moreover, the similarity of the responses in monkeys, tree shrews, guinea pigs and chicks to hemi-retinal form deprivation indicates that the presence of a well-developed fovea does not diminish the contribution of these local retinal mechanisms to ocular growth, that the nature of these spatially localized mechanisms are fundamental from an evolutionary perspective, and that it is likely that similar mechanisms exist in humans.

The obvious nasal-temporal asymmetries in the shape of the posterior globe that were observed in many of our treated monkeys were very similar to findings in chicks.5,13 However, given the anatomical differences between the scleras of chicks and monkeys, the prominent structural changes in our infant monkeys were somewhat surprising. In chicks, the local axial elongation produced by hemi-retinal form deprivation causes the treated portion of the globe to bulge out. This is not a surprising finding in chicks because their scleras are relatively rigid, being composed primarily of a cartilaginous layer that actively grows during vision-induced axial elongation.35,36 In comparison, the scleras of monkeys consist primarily of fibrous connective tissue that is generally considered to be softer and more pliable than the chick sclera and axial elongation is thought to come about as a consequence of remodeling of scleral tissue that leads to stretching in the tangential direction.37–39 In this respect, it could be argued that selective peripheral form deprivation or hemi-retinal form deprivation would result in a more prolate shaped eye in monkeys and that any discreet bulges would, in essence, be smoothed out. However, the distinctive, local changes in posterior globe curvature observed in our MRI scans show that, at least in developing eyes, the monkey sclera can hold its shape. These results suggest that different types of visual experience could produce a range of distinctly different shaped eyes in primates similar to those that have been observed in chicks.40

Monocular experimental manipulations of vision have been shown to produce bilateral effects in several species of laboratory animals. For example, the refractive errors for the fellow, non-treated eyes of monkeys that undergo full-field form deprivation can be more myopic or more hyperopic than normal eyes.19,20,41 In this respect, several observations indicate that the

NFDs produced interocular effects in our monkeys. In particular, in several monkeys, the fellow, non-treated eyes developed atypical central refractive errors and/or abnormal patterns of peripheral refractions. For example, at the end of the treatment period, the non-treated eye's central refraction for monkey MON 368 (middle row, Figure 2) was more hyperopic than that for any age-matched normal monkey, however, the pattern of peripheral refractive errors was not obviously altered. More interestingly, two of the three monkeys that failed to develop nasal field myopia in their treated eyes demonstrated obvious nasal-temporal asymmetries in the pattern of peripheral refractions in their fellow, non-treated eyes. In both cases (MKY GEN 359 and MKY MIT 367), the nasal-temporal asymmetries were larger in the fellow eyes than in the treated eyes and the fellow eyes showed degrees of nasal field myopia that were outside the range of relative peripheral refractions observed in the normal monkeys.

The nature of the mechanisms responsible for interocular effects is not well understood. It has been hypothesized that interocular effects may be mediated by humoral factors and/or central influences of some kind, possibly via innervations to the choroid.8,19,20,41,42 It is also possible that in some cases the interocular effects are vision-induced. For example, because accommodation is yoked in the two eyes of primates, rearing conditions that alter the accommodation of one eye (e.g., anisometropic treatment lenses) will potentially influence the level of accommodation in the fellow eye and potentially its refractive development, depending on which eye the animal uses to fixate objects.23 Similarly, conditions such as monocular form deprivation that prevent binocular vision could, by altering convergence-accommodative interactions, change the accommodative behavior of the fixating fellow eye and eventually the refractive development of that eye.20

It seems unlikely that any of these possibilities, which would be expected to have global effects on the fellow eye, are responsible for the nasal-temporal asymmetries observed in the fellow eyes of some of our NFD monkeys. Although it is possible that a yet unknown central mechanism could produce selective regional changes in eye growth, we speculate that the fellow eye asymmetries could reflect alterations in the fixation behavior of the NFD monkeys and the effects of visual experience. We have assumed that the NFD animals would prefer to fixate primarily via the non-treated eye. However, perhaps a small number of the treated monkeys choose, for whatever reason, to fixate with their treated eyes. Logically these animals would rotate their treated eyes in the temporal direction to maximize that eye's central field of view, which would likely result in a concomitant versional eye movement of the fellow eye in the nasal direction. Chronic nasal deviation could have resulted in a selective reduction in the image quality in the temporal retina of the fellow eye. In other words, by selectively fixating with the treated eyes, a nasal-temporal asymmetry in retinal image quality may have been transferred to the fellow eye.

The existence of independent, vision-dependent mechanisms that integrate visual information over restricted retinal regions has important implications for the role of vision in the genesis of common refractive errors and for potential optical treatment regimens for refractive error. First, because the refractive state at the fovea is dependent on ocular changes at the posterior pole and in the periphery (i.e., an expansion of the sclera in the periphery would displace the central retina in a posterior direction along the visual axis), peripheral visual signals can influence central refractive development in a manner that is independent of the nature of central vision. In this respect, there is growing evidence that the pattern of peripheral refractive errors in humans can influence central refractive development.40,43,44 Moreover, we have previously shown that selective peripheral form deprivation28,34 and relative peripheral hyperopic defocus (Smith, *IOVS*, 2007,48, ARVO e-Abstract 1533) can promote central axial elongation and central myopia in infant monkeys, even in the presence of unrestricted central vision. However, because local retinal mechanisms operate in an independent manner and because vision-induced changes in the growth rate of the peripheral globe will influence central

axial length, it should also be possible to influence central refractive development in a therapeutic manner by manipulating only peripheral vision. For example, to reduce myopia progression, it should be possible to eliminate peripheral visual signals that promote axial elongation and/or provide peripheral visual signals that normally slow ocular growth without changing or interfering with central vision. The key point is that one should be able to design a correcting lens to provide optimal central vision and, at the same time, a peripheral visual signal to reduce or accelerate central axial growth.

Acknowledgments

This work was supported by NIH Grants EY-03611, EY-07551, and RR-17205 and funds from the Vision CRC and the UH Foundation.

References

1. Smith, EL, III. Environmentally induced refractive errors in animals. In: Rosenfield, M.; Gilmartin, B., editors. Myopia and Nearwork. Oxford: Butterworth-Heinemann; 1998. p. 57-90.
2. Wallman J, Winawer J. Homeostasis of eye growth and the question of myopia. Neuron 2004;43:447–468. [PubMed: 15312645]
3. Norton TT. Animal Models of Myopia: Learning How Vision Controls the Size of the Eye. Inst Lab Anim Res J 1999;40:59–77.
4. Norton TT, Essinger JA, McBrien NA. Lid-suture myopia in tree shrews with retinal ganglion cell blockade. Vis Neurosci 1994;11:143–153. [PubMed: 8011577]
5. Troilo D, Gottlieb MD, Wallman J. Visual deprivation causes myopia in chicks with optic nerve section. Curr Eye Res 1987;6:993–999. [PubMed: 3665562]
6. Wildsoet C, Pettigrew JD. Experimental myopia and anomalous eye growth patterns unaffected by optic nerve section in chickens. Evidence for local control of eye growth 1988;3:99–107.
7. Troilo D, Wallman J. The regulation of eye growth and refractive state: An experimental study of emmetropization. Vision Res 1991;31:1237–1250. [PubMed: 1891815]
8. Wildsoet C, Wallman J. Choroidal and scleral mechanisms of compensation for spectacle lenses in chicks. Vision Res 1995;35:1175–1194. [PubMed: 7610579]
9. Wildsoet CF. Neural pathways subserving negative lens-induced emmetropization in chicks - Insights from selective lesions of the optic nerve and ciliary nerve. Curr Eye Res 2003;2003:371–385. [PubMed: 14704921]
10. Diether S, Schaeffel F. Local changes in eye growth induced by imposed local refractive error despite active accommodation. Vision Res 1997;37:659–668. [PubMed: 9156210]
11. Hodos W, Kuenzel WJ. Retinal-image degradation produces ocular enlargement in chicks. Invest Ophthalmol Vis Sci 1984;25:652–659. [PubMed: 6724835]
12. Wallman J, Adams JI. Developmental aspects of experimental myopia in chicks: Susceptibility, recovery and relation to emmetropization. Vision Res 1987;27:1139–1163. [PubMed: 3660666]
13. Wallman J, Gottlieb MD, Rajaram V. Fugate-Wentzek L. Local retinal regions control local eye growth and myopia. Science 1987;237:73–77. [PubMed: 3603011]
14. Norton TT, Siegwart JT. Local myopia produced by partial visual-field deprivation in tree shrew. Soc Neurosci Abstr 1991;17:558.
15. Hodos W, Erichsen J. Lower-field myopia in birds: An adaptation that keeps the ground in foucs. Vision Res 1990;30:653–657. [PubMed: 2378058]
16. Miles FA, Wallman J. Local ocular compensation for imposed local refractive error. Vision Res 1990;30:339–349. [PubMed: 2336793]
17. Raviola E, Wiesel TN. An animal model of myopia. N Eng J Med 1985;312:1609–1615.
18. Smith EL III, Harwerth RS, Crawford MLJ, von Noorden GK. Observations on the effects of form deprivation on the refractive status of the monkey. Invest Ophthalmol Vis Sci 1987;28:1236–1245. [PubMed: 3610541]

19. Smith EL III, Hung L-F. Form-deprivation myopia in monkeys is a graded phenomenon. Vision Res 2000;40:371–381. [PubMed: 10820617]
20. Smith EL III, Hung L-F, Kee C-s, Qiao Y. Effects of brief periods of unrestricted vision on the development of form-deprivation myopia in monkeys. Invest Ophthalmol Vis Sci 2002;43:291–299. [PubMed: 11818369]
21. Tigges M, Tigges J, Fernandes A, Eggers HM, Gammon JA. Postnatal axial eye elongation in normal and visually deprived rhesus monkeys. Invest Ophthalmol Vis Sci 1990;31:1035–1046. [PubMed: 2354909]
22. Smith EL III, Huang J, Hung L-F, Ramamirtham R, Blasdel T, Humbird T, Bockhorst K. Hemi-retinal form deprivation and refractive development in monkeys. American Academy of Optometry Anaheim, USA: Abstract 80005. 2008
23. Smith EL III, Hung L-F. The role of optical defocus in regulating refractive development in infant monkeys. Vision Res 1999;39:1415–1435. [PubMed: 10343811]
24. Qiao-Grider Y, Hung L-F, Kee C-s, Ramamirtham R, Smith E III. Normal ocular development in young rhesus monkeys (*Macaca mulatta*). Vision Res 2007;47:1424–1444. [PubMed: 17416396]
25. Huang J, Hung L-F, Ramamirtham R, Blasdel T, Humbird T, Bockhorst K, Smith EL III. Form deprivation alters peripheral refractions and ocular shape in infant rhesus monkeys (*Macaca mulatta*). Invest Ophthalmol Vis Sci. 2009in press
26. Qiao-Grider Y, Hung L-F, Kee C-s, Ramamirtham R, Smith EL III. A comparison of refractive development between two subspecies of infant rhesus monkeys (*Macaca mulatta*). Vision Res 2007;47:1424–1444. [PubMed: 17416396]
27. Smith EL III, Harwerth RS, Wensveen JM, Ramamirtham R, Kee C-s, Hung L-F. Effects of brief daily periods of unrestricted vision on the development of form-deprivation myopia in monkeys. Invest Ophthalmol Vis Sci 2002;43:291–299. [PubMed: 11818369]
28. Smith EL III, Kee C-s, Ramamirtham R, Qiao-Grider Y, Hung L-F. Peripheral vision can influence eye growth and refractive development in infant monkeys. Invest Ophthalmol Vis Sci 2005;46:3965–3972. [PubMed: 16249469]
29. Hung L-F, Ramamirtham R, Huang J, Qiao-Grider Y, Smith E III. Peripheral refraction in normal infant rhesus monkeys. Invest Ophthalmol Vis Sci 2008;49:3747–3757. [PubMed: 18487366]
30. Harris WF. Algebra of sphero-cylinders and refractive errors, and their means, variance, and standard deviation. Am J Optom Physiol Opt 1988;65:794–902. [PubMed: 3207150]
31. Rempt R, Hoogerheide J, Hoogenboom WPH. Peripheral retinoscopy and the skiagram. Ophthalmologica 1971;162:1–10. [PubMed: 5547863]
32. Kee, C-s; Hung, L-F.; Qiao, Y.; Habib, A.; Smith, EL, III. Prevalence of astigmatism in infant monkeys. Vision Res 2002;42:1349–1359. [PubMed: 12044741]
33. Schaeffel F, Hagel G, Bartmann M, Kohler K, Zrenner E. 6-Hydroxydopamine does not affect lens-induced refractive errors but suppresses deprivation myopia. Vision Res 1994;34:143–149. [PubMed: 8116274]
34. Smith EL III, Ramamirtham R, Qiao-Grider Y, Hung L-F, Huang J, Kee C-s, Coats D, Paysee E. Effects of foveal ablation on emmetropization and form-deprivation myopia. Invest Ophthalmol Vis Sci 2007;48:3914–3922. [PubMed: 17724167]
35. Christensen AM, Wallman J. Evidence that increased scleral growth underlies visual deprivation myopia in chicks. Invest Ophthalmol Vis Sci 1991;32:2143–2150. [PubMed: 2055705]
36. Rada JA, Thoft RA, Hassel JR. Increased aggrecan (cartilage proteoglycan) production in the sclera of myopic chicks. Dev Biol 1991;147:303–312. [PubMed: 1916012]
37. Guggenheim JA, McBrien NA. Form-deprivation myopia induces activation of scleral matrix metalloproteinase-2 in tree shrew. Invest Ophthalmol Vis Sci 1996;37:1380–1395. [PubMed: 8641841]
38. Norton TT, Rada JA. Reduced extracellualar matrix accumulation in mammalian sclera with induced myopia. Vision Res 1995;35:1271–1281. [PubMed: 7610587]
39. Siegwart JT, Norton TT. Regulation of the mechanical properties of tree shrew sclera by the visual environment. Vision Res 1999;39:387–407. [PubMed: 10326144]
40. Stone RA, Flitcroft DI. Ocular shape and myopia. Ann Acad Med Singapore 2004;33:7–15. [PubMed: 15008555]

41. Bradley DV, Fernandes A, Boothe RG. The refractive development of untreated eyes of rhesus monkeys varies according to the treatment received by their fellow eyes. Vision Res 1999;39:1749–1757. [PubMed: 10343866]

42. Kiorpes L, Wallman J. Does experimentally-induced amblyopia cause hyperopia in monkeys? Vision Res 1995;35:1289–1297. [PubMed: 7610589]

43. Hoogerheide J, Rempt F, Hoogenboom WP. Acquired myopia in young pilots. Ophthalmologica 1971;163:209–215. [PubMed: 5127164]

44. Mutti DO, Sholtz RI, Friedman NE, Zadnik K. Peripheral refraction and ocular shape in children. Invest Ophthalmol Vis Sci 2000;41:1022–1030. [PubMed: 10752937]

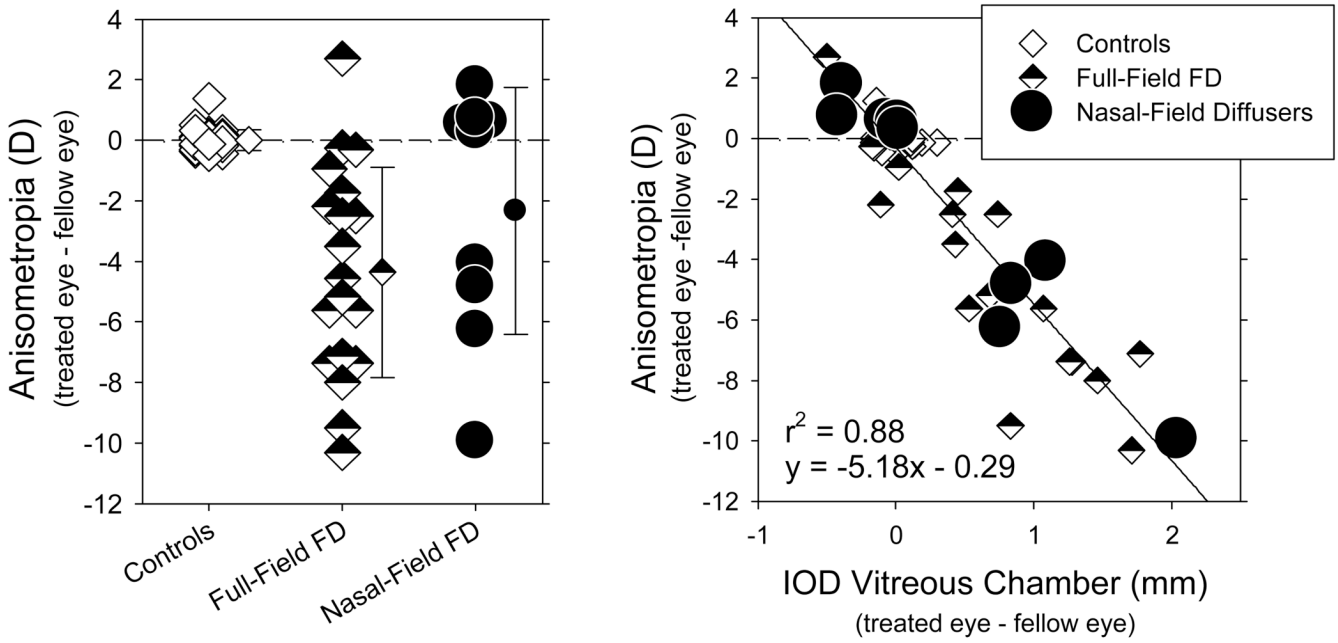

FIGURE 1.

Left. Interocular differences in spherical-equivalent refractive corrections measured along the pupillary axis for individual control (normal monkeys reared with unrestricted vision and monkeys reared with zero-powered lenses over both eyes) and treated monkeys (right or treated eye – left or fellow eye). The means ± 1 SD are shown to the right of the individual data. The measurements were made at the end of the period of form deprivation or around 150 days of age for the control monkeys. All of the treated animals wore the same strength of diffusers (i.e., “LP” occlusion foils). Animals in the Full-Field FD group wore diffusers that degraded image quality across the entire visual field continuously throughout the treatment period. The Nasal-Field FD group also wore diffusers continuously; however these diffusers only affected image quality in the nasal visual field. Right. Interocular differences in refractive error plotted as a function of the interocular differences in vitreous chamber depth for the individual animals represented in the left panel. The data for the full-field FD and the FD + normal vision groups have been re-plotted from Smith et al.19,20 and Huang et al..25

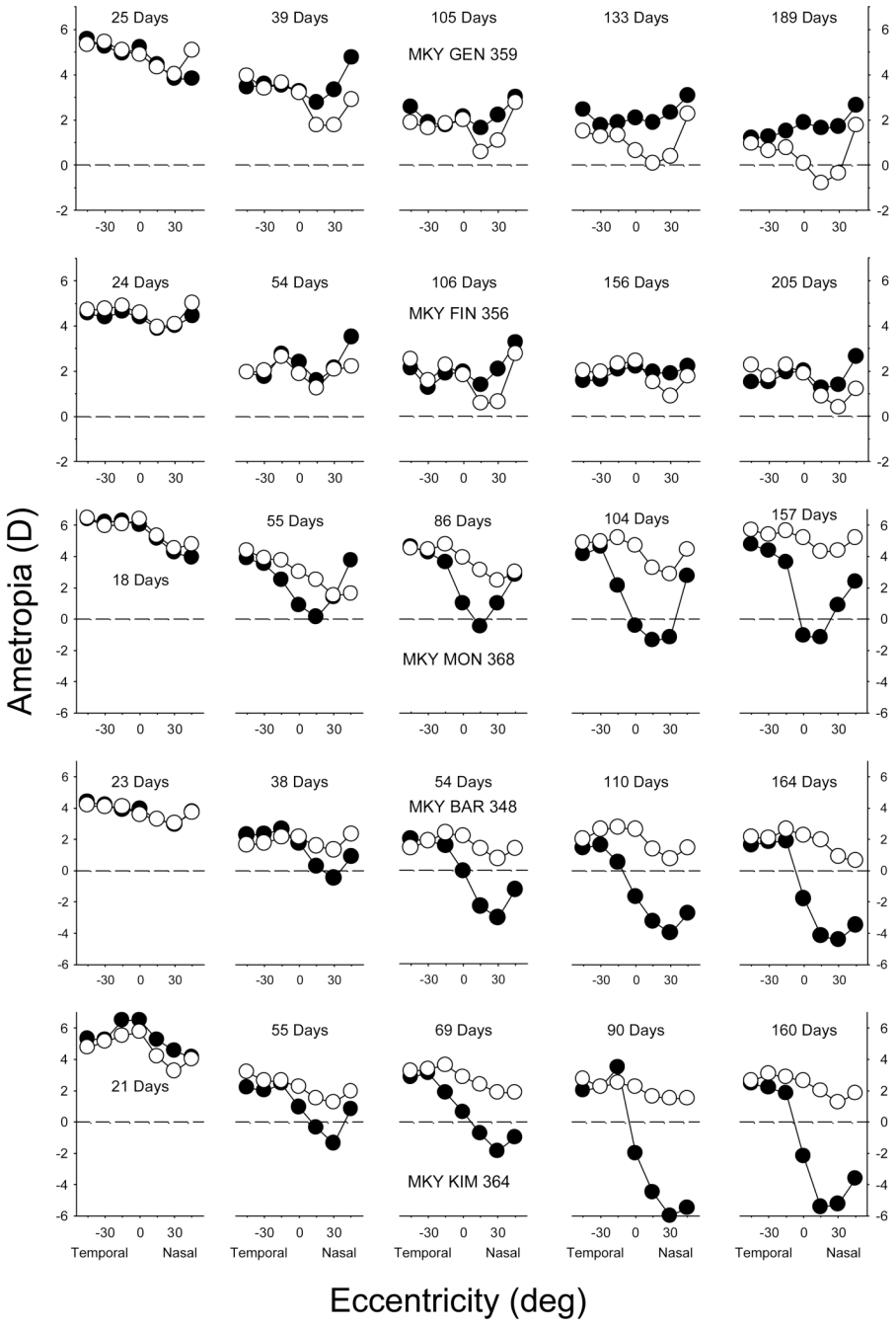

Figure 2.

Spherical-equivalent refractive corrections that were obtained at different times during the treatment period for 5 representative monkeys reared with nasal-field diffusers plotted as a function of visual field eccentricity along the horizontal meridian. The plots on the left were obtained at the onset of the treatment period; the ages for the subsequent measures are shown in each plot. Zero eccentricity represents the pupillary axis. The filled and open symbols represent the treated and fellow eyes, respectively.

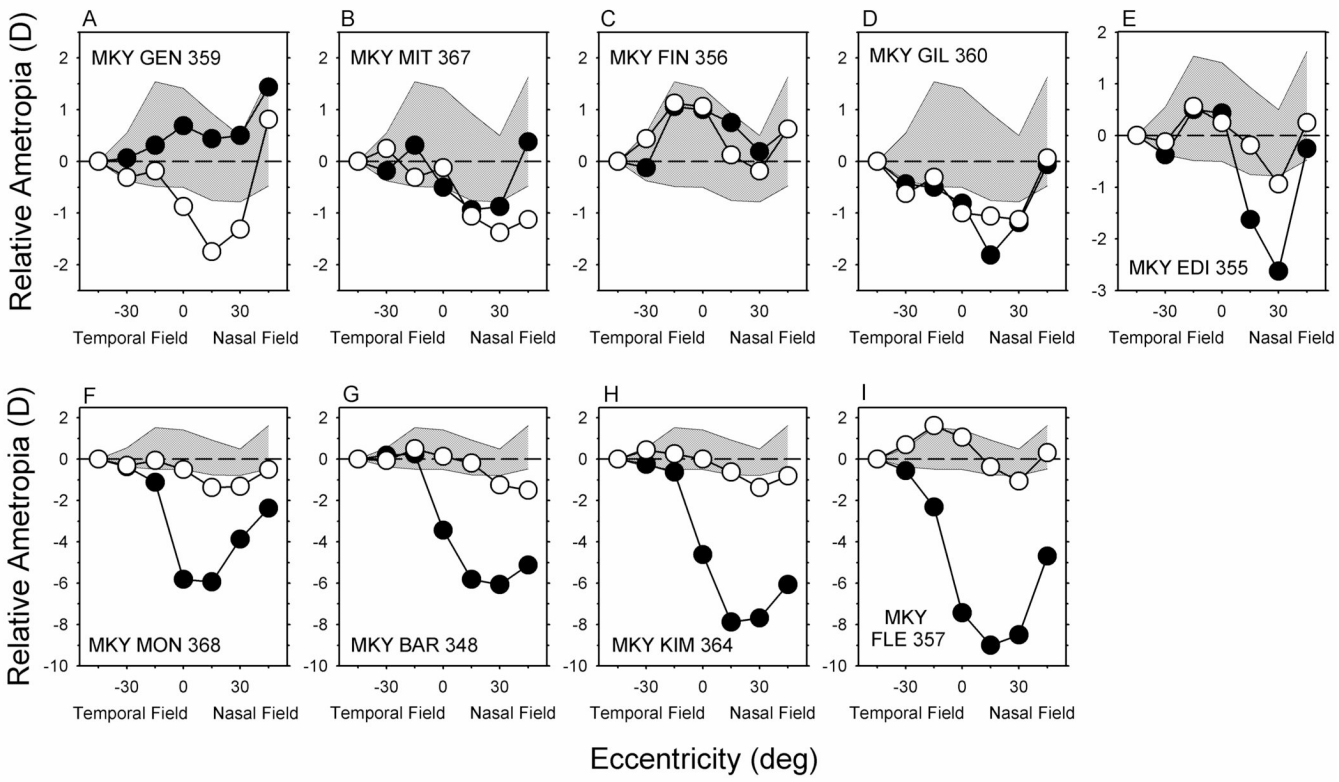

FIGURE 3.

Relative ametropias plotted as a function of visual field eccentricity along the horizontal meridian for individual monkeys reared with nasal-field diffusers. The data were obtained at the end of the treatment period and have been normalized to the refractive correction measured at the 45° temporal field eccentricity. The filled and open symbols represent the treated and fellow eyes, respectively. The shaded areas represent ±1 SD from the mean relative ametropias for the right eyes of 7 normal monkeys. The data for 6 of the normal monkeys have been re-plotted from Hung et al.29 and Huang et al..25

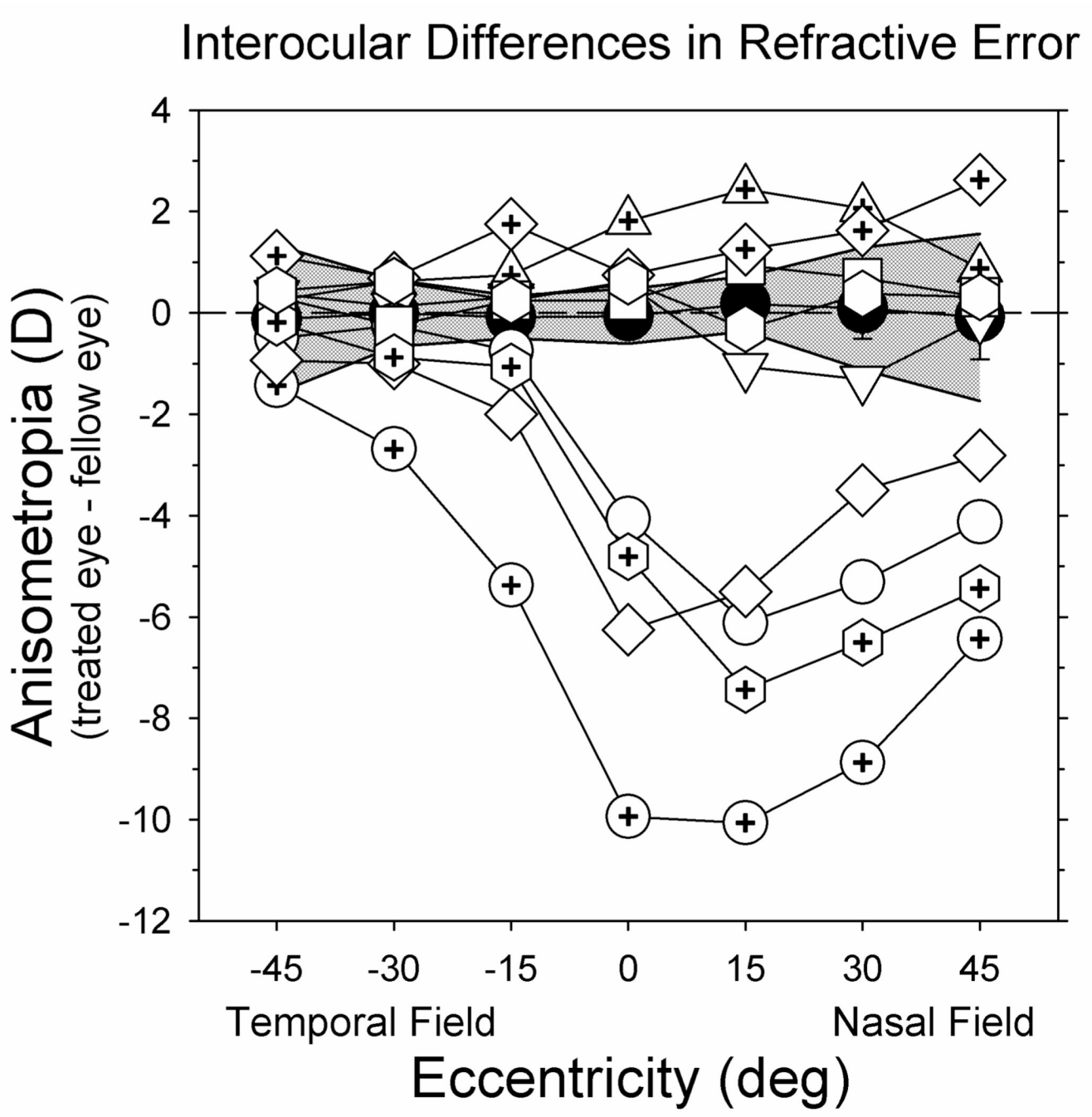

FIGURE 4.

Interocular differences in spherical-equivalent refractive corrections (right or treated eye – left or fellow eye) obtained at the end of the treatment period plotted as a function of horizontal visual field eccentricity for individual monkeys reared with nasal-field diffusers (open symbols). The filled symbols and the shaded area represent, respectively, the mean interocular differences in refractive corrections and ±2 SDs from the means for 7 normal monkeys. The data for 6 of the normal monkeys have been re-plotted from Hung et al.29 and Huang et al..25

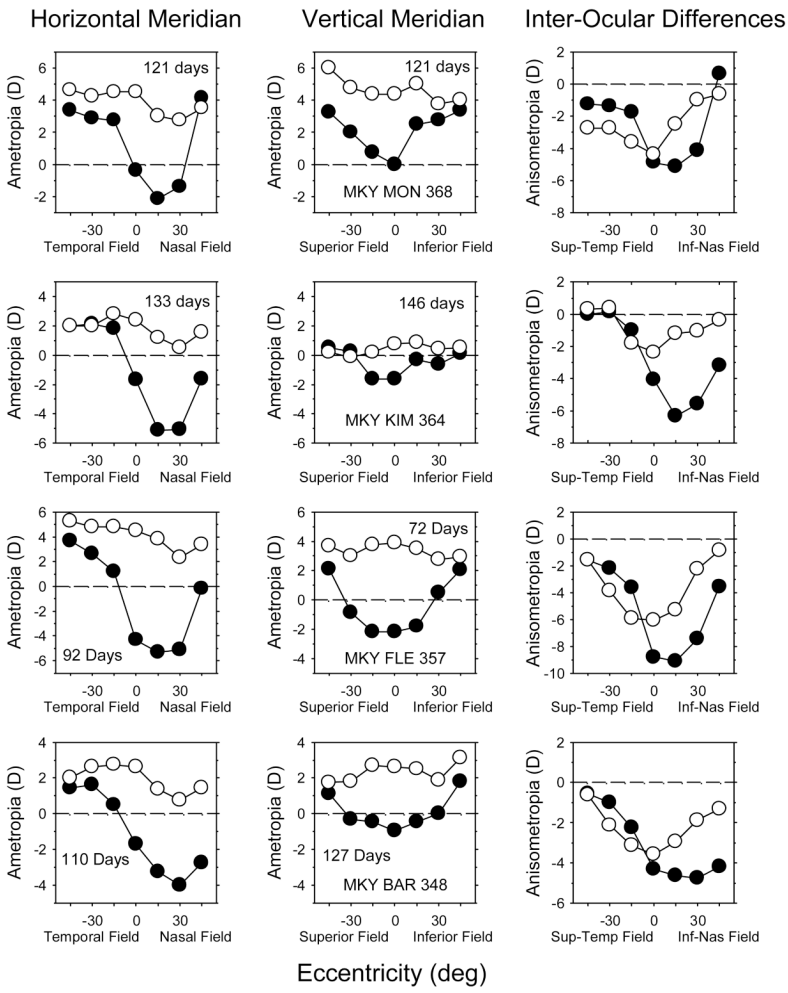

FIGURE 5.

Comparisons of the pattern of peripheral refractions along the horizontal (left column) and vertical meridians (middle column) for 4 representative monkeys reared with nasal-field diffusers. The filled and open symbols represent the treated and fellow eyes, respectively. The age at the time of the measurement is shown in each plot. The right column shows the interocular differences in refractive corrections (treated eye – fellow eye) plotted as a function of eccentricity for the horizontal (filled symbols) and vertical meridians (open symbols).

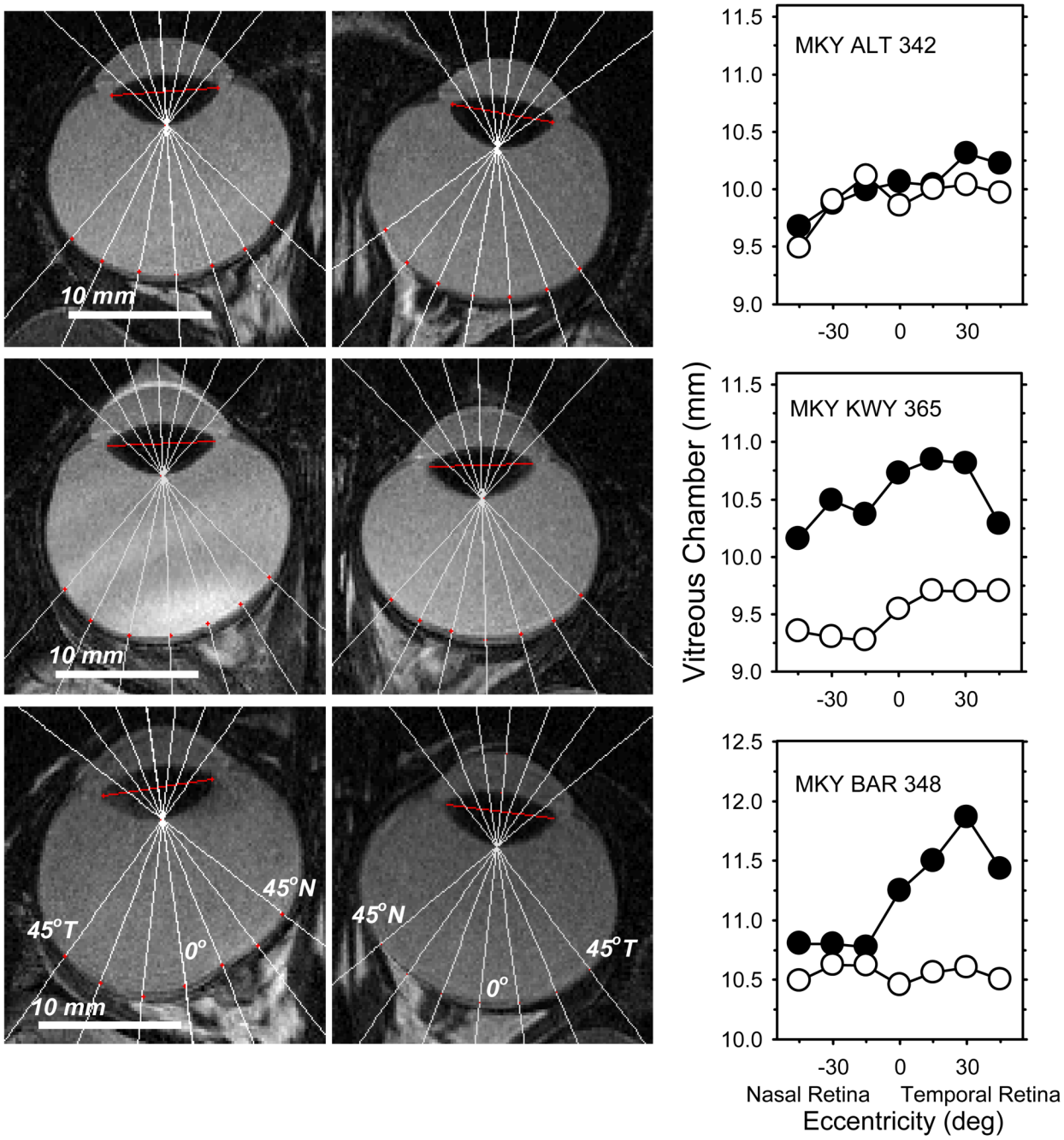

FIGURE 6.

Left. Magnetic resonance images obtained in the horizontal plane at ages corresponding to the end of the diffuser-rearing period for both eyes of a normal control monkey (top), a FFD monkey with central form deprivation myopia (middle), and a NFD monkey that developed a relatively high degree of nasal field myopia (bottom). For the FFD and NFD monkeys, the treated eyes are shown on the left. Right. Vitreous chamber depth plotted as a function of eccentricity for the right / treated (filled circles) and left / fellow eyes (open circles). The normal and FFD monkey data were presented previously in Huang et al..25

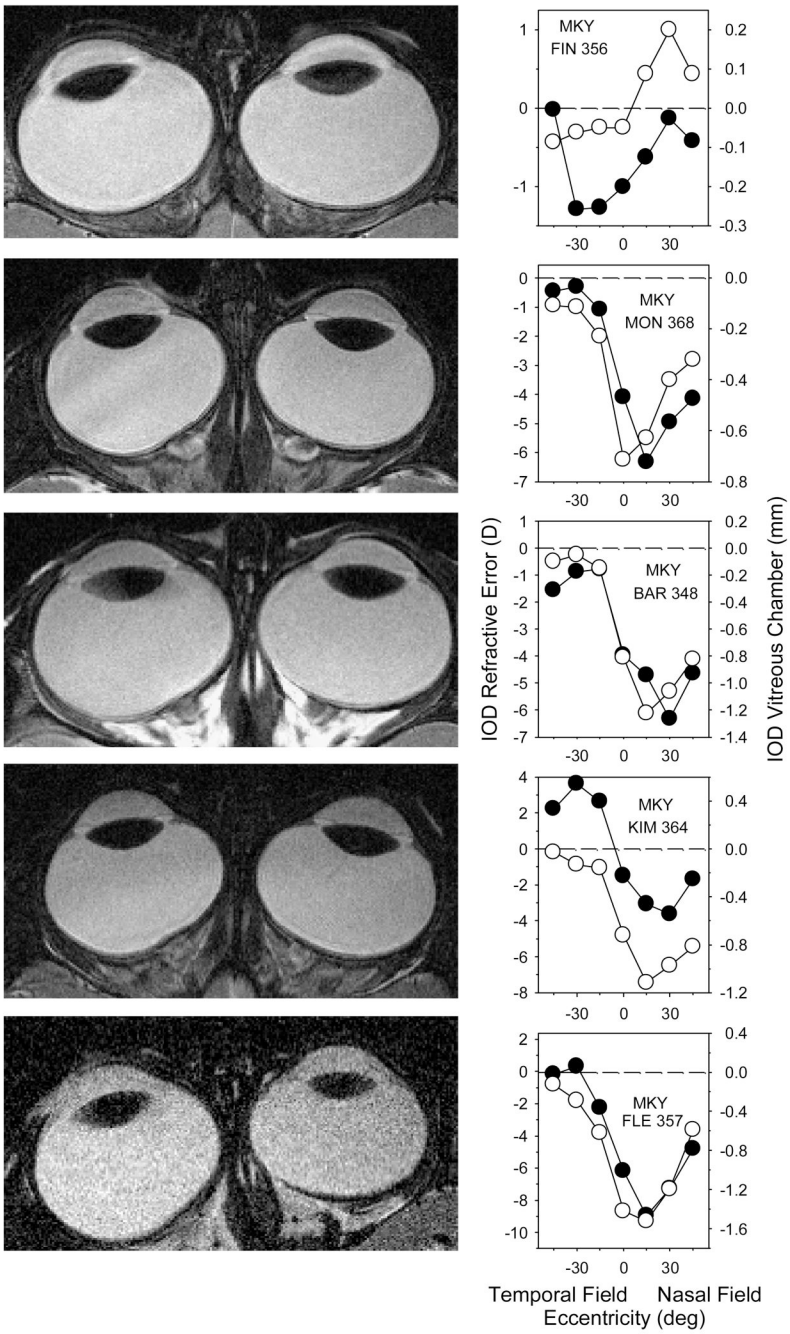

FIGURE 7.

Magnetic resonance images (left) and comparisons of the interocular differences in refractive corrections (open symbols and left ordinate scale; treated eye – fellow eye) and vitreous chamber depth (filled symbols and right ordinate scale; fellow eye – treated eye) as a function of horizontal eccentricity (right) for 5 representative monkeys reared with nasal-field diffusers (rows). The MR images were obtained in the axial plane near the end of the treatment period. The treated eyes are shown on the left.

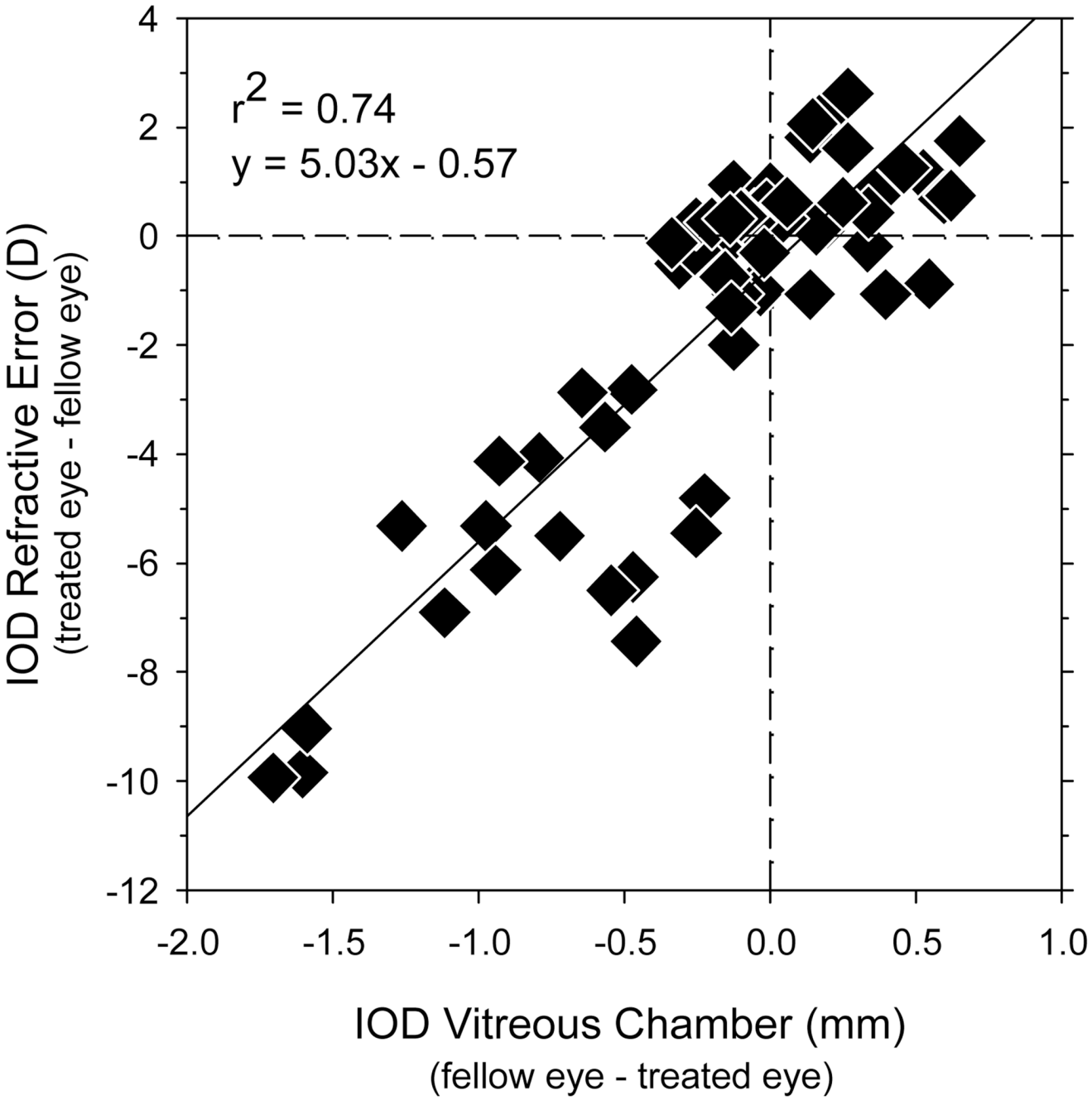

Figure 8.
Interocular differences in refractive error (treated eye – fellow eye) plotted as a function of the interocular differences in vitreous chamber depth determined from the MR images (fellow eye –treated eye). Data are shown for all NFD-reared monkeys and for all eccentricities along the horizontal meridian. The solid line represents the best fitting regression line.

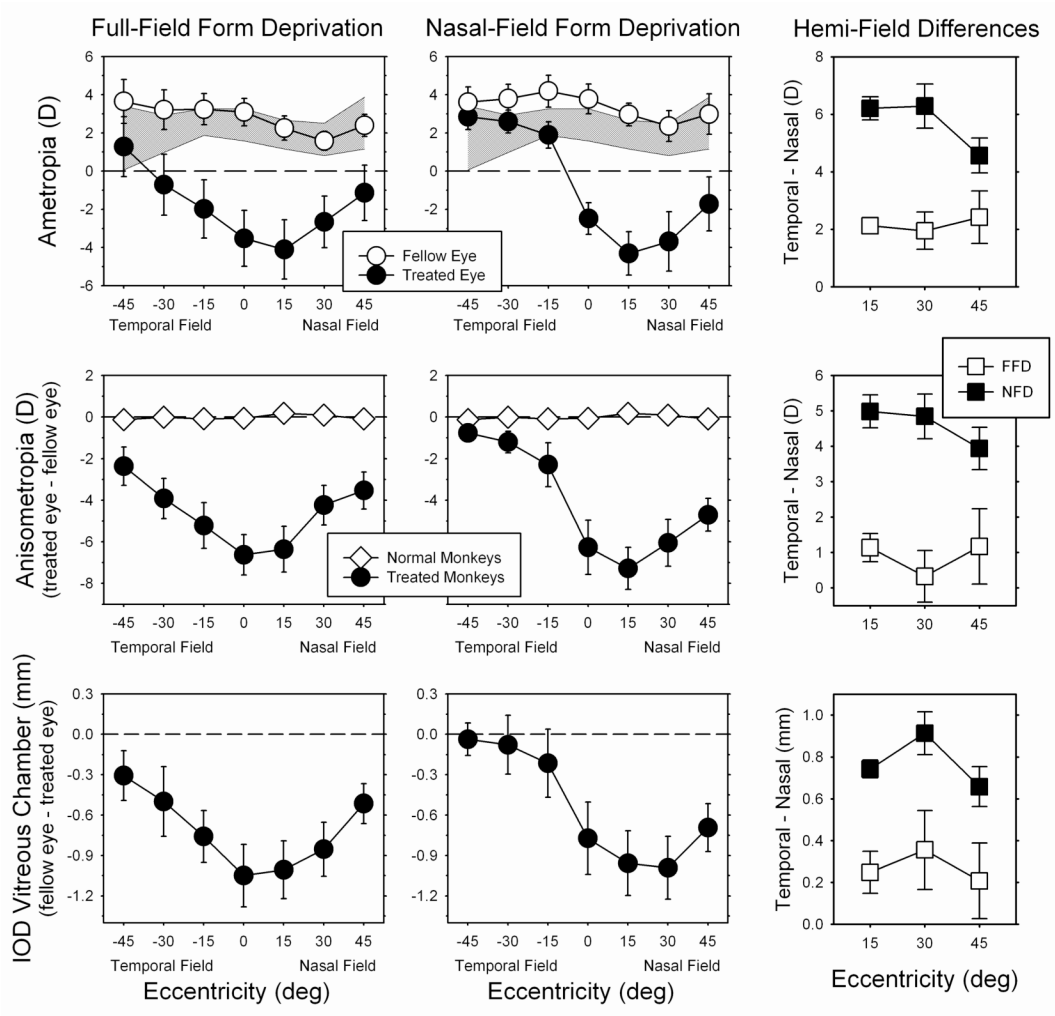

FIGURE 9.

Comparisons of the average (± SE) absolute refractive errors (top; treated eye = filled symbols, fellow eye = open symbols), degree of anisometropia (middle; treated monkeys = filled symbols, control monkeys = open symbols), and interocular differences in vitreous chamber depth (bottom) plotted as a function of horizontal visual field eccentricity. Data are shown in the left column for 6 monkeys that were reared with full-field diffusers and that developed central form-deprivation myopia. The results for the 4 NFD monkeys that showed the largest myopic changes are shown in the middle column. The right column shows the differences in the nasal and temporal hemi field results (temporal field – nasal field) plotted as a function of eccentricity for the FFD (open squares) and NFD monkeys (filled squares) In the top plots, the shaded area represents ±2 SDs from the mean for the normal monkeys (n = 7). The data for the FFD monkeys and 6 of the normal monkeys have been re-plotted from Huang et al.25